Pattern Recognition Report

Yash Belur, Tam Amabibi
yb521 (02100668,), ta1524 (06011762)

A. Data Preparation and Visualisation

A.1. Plotting Movement

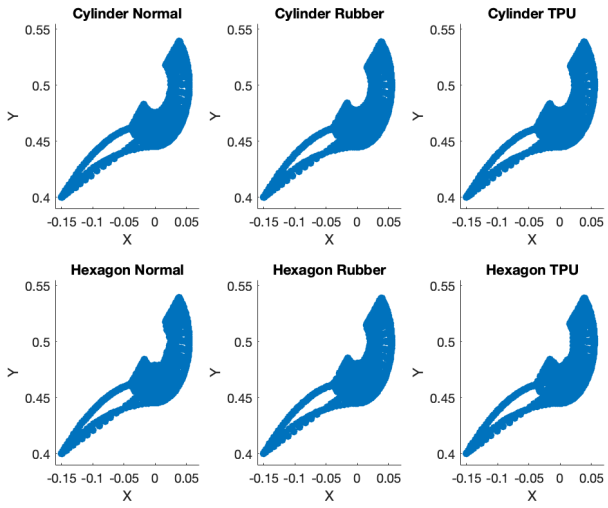

Figure 1: Movement Trajectory of End Effector

In this section, we analyse the movement trajectories of the UR5e robot's end effector when interacting with cylinder and hexagon-shaped objects. The recorded end-effector positions were extracted and visualised to observe any differences in movement patterns.

Figure 1 illustrates the movement trajectory of the robot's end effector for various material configurations of the cylinder and hexagon objects, showing how the robot approaches and makes contact with them. While the overall trajectory shape remains consistent across different materials, reflecting stable robotic control, variations in end effector positioning near the contact regions suggest differences in material compliance.

These observations suggest that material properties do not influence the robot's contact interaction, which may be useful for subsequent pattern recognition tasks.

A.2. Peak Normal Contact Force

Figure 2 shows the peak normal contact force of the sensor and their Time Index.

A.3. Papillae Data

For the three cylinders (normal, TPU, and rubber), a 3D scatter plot was generated using the force data from the middle papillae (P4). The force vectors in the X, Y, and Z directions were plotted using different colours for each object.

From Figure 3, we can observe that the force distributions vary among the three materials. The rubber cylinder appears to have higher variance along the Z-axis, indicating differences in material deformation under contact forces. A similar 3D scatter plot was generated for one of the corner papillae. The results are shown below 4.

Comparing Figures 3 and 4 reveals several key differences in the force data distribution. The middle papillae show a more pronounced spread, while the corner papillae exhibit greater variation in the X and Y directions. The rubber cylinder data displays higher variance in both regions, though the distribution is less centralized in the corner papillae. In contrast, the TPU and normal cylinders have more compact distributions in the middle papillae, indicating a more localized response to applied forces.

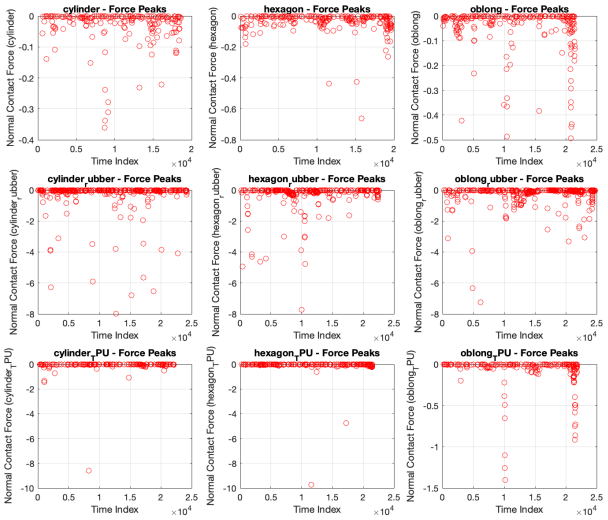

Figure 2: Peak Normal Contact Data

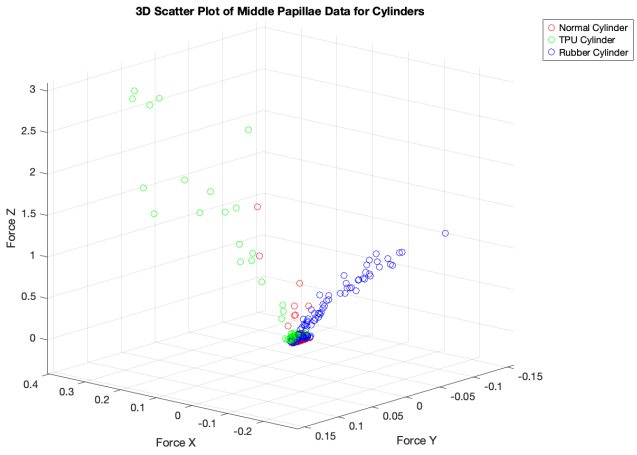

Figure 3: Middle Papillae Force Data

These differences stem from the distinct mechanical properties of the materials and the varying placement of the papillae. The middle papillae experience more uniform contact forces, while the corner papillae are subject to shear and rotational forces, resulting in a broader spread of force data.

B. Principal Component Analysis

B.1. Middle Sensor PCA

The force data from the middle sensor of the three cylindrical objects was standardized and plotted with the principal components displayed in Figure 5.

The principal components are shown as arrows indicating the directions of greatest variance in the data. The first principal component (PC1) captures the most variance, followed by PC2 and PC3.

The data was then reduced to two dimensions using PCA, and the resulting distribution is shown in Figure 6. From this figure, we can see that the data separates into distinct clusters based on material type, indicating that PCA effectively captures variance in force patterns among the different cylinders.

Figure 7 displays the variance across the first three principal components,

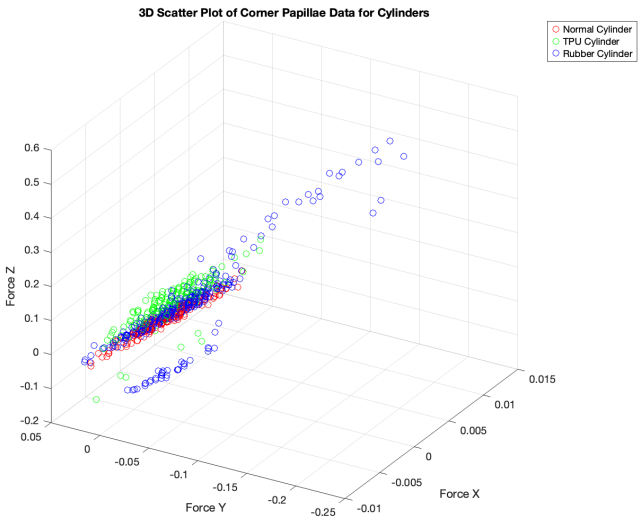

Figure 4: Corner Papillae Force Data

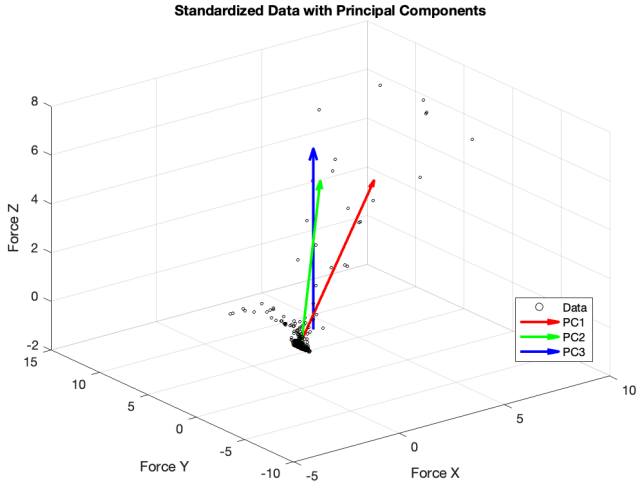

Figure 5: Visualisation of Principles Components of Middle Sensor

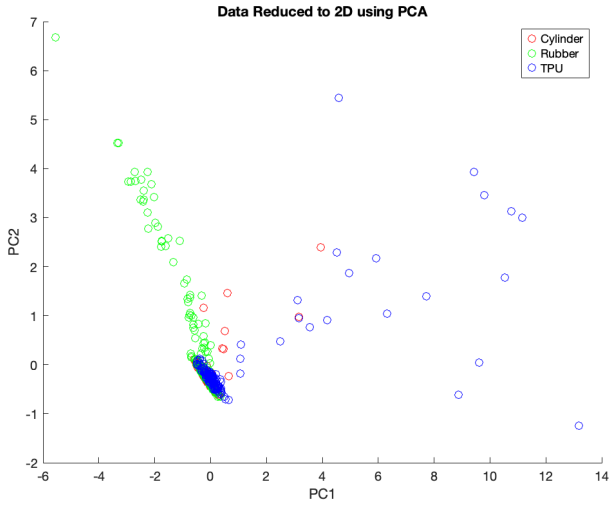

Figure 6: Data reduced to two Dimensions

where PC1 captures the majority of the variance, while PC2 and PC3 contain smaller yet meaningful variations in force data. The PCA results demonstrate that force data from the middle sensor can be effectively represented in a lower-dimensional space without losing significant information. The 2D PCA plot

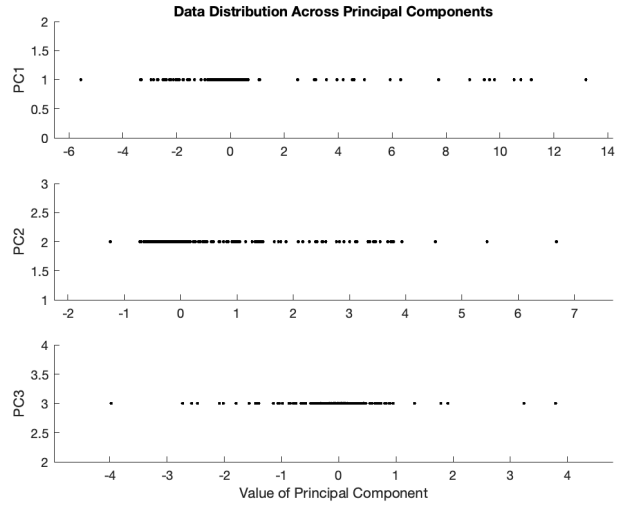

Figure 7: 1D Number Lines of Data Distribution across Principle Components

reveals that different material types exhibit distinct force characteristics, indicating the feasibility of material classification using PCA.

The first principal component contains most of the variance, making it the most informative direction for distinguishing between materials. The clear separation between clusters in the 2D plot highlights how PCA preserves material-specific force distribution patterns, reinforcing its value as a dimensionality reduction technique for tactile data analysis. Furthermore, the 1D distribution plot confirms this, with PC1 dominating the variance and PC2 and PC3 contributing less. This suggests that the most discriminative information resides in PC1, validating PCA's effectiveness in summarizing this dataset.

B.2. All Sensors PCA

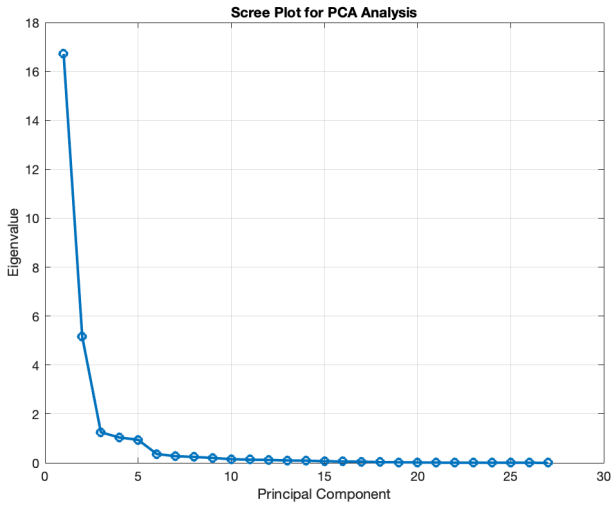

Figure 8: Scree Plot of Variance of all Principle Components

A scree plot was generated to analyse the variance explained by each principal component. This helps in determining the number of components to retain. From Figure 8, we can observe that the majority of the variance is explained by the first few principal components, indicating that dimensionality reduction can be effectively applied without significant loss of information.

The distribution of the data along the first three principal components is visualised in Figure 9. This Figure demonstrates how data is spread across the principal components. The first principal component captures the most variance, while subsequent components contribute progressively less.

The data was further reduced to two dimensions using PCA, as shown in Figure 10. From this projection, it is clear that PCA effectively clusters different material types while maintaining meaningful separation, demonstrating its

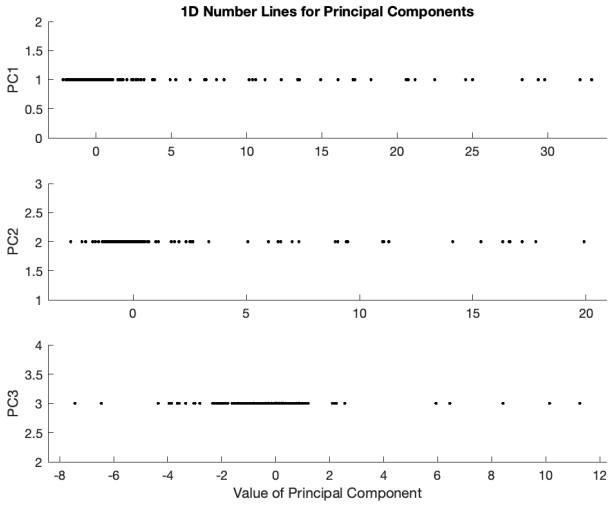

Figure 9: 1D Number Lines across first three Principle Components

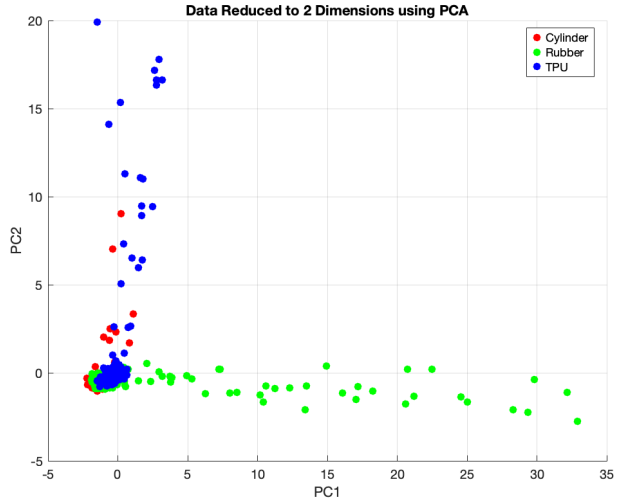

Figure 10: Data Reduced to two Dimensions

suitability for dimensionality reduction. Including all papillae in the analysis provides a more comprehensive representation of object interactions by capturing forces distributed across various contact points. The scree plot indicates that only a few principal components account for most of the variance, suggesting that incorporating all papillae may introduce redundancy without significantly improving classification accuracy.

The 1D number line visualisation reveals that while PC1 captures the majority of the variance, additional components offer finer detail, which could enhance object differentiation. The 2D PCA plot confirms that including all papillae improves the separation between material types, though this comes at the cost of increased computational complexity. However, this approach carries the risk of over-fitting when applying classification models, as minor variations in contact forces across sensors might introduce noise rather than useful information.

In contrast, using only P4—the middle papilla—simplifies the analysis and reduces computational demands while still capturing meaningful trends. Yet, this simplification may overlook subtle force variations that could contribute to more accurate object differentiation. Balancing these trade-offs is critical for optimizing the analysis while maintaining computational efficiency and avoiding potential pitfalls like over-fitting.

C. Linear Displacement Analysis

The aim of this task was to see if the same shape object made of two materials through the central papillae displacement can be discriminated against using Linear Discriminate Analysis. To present show how LDA works, the data of the oblong TPU and rubber objects are loaded into MATLAB. Using this data, the tactile displacement is extracted then visualised on a 3D scatter graph.

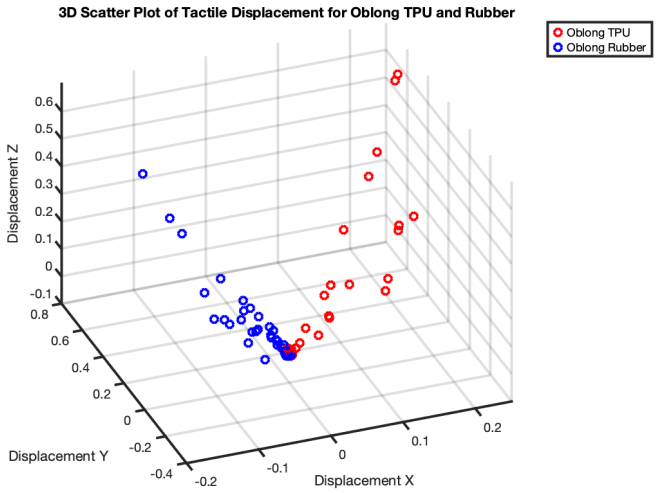

Figure 11: The visualisation of Tactile Displacement of the two Materials

Figure 11 shows the visualisation of tactile displacement of the oblong TPU and rubber materials on a 3D scatter plot, using red and blue dots as legends respectively. The observations made when plotted show that the two materials are distinguishable. In terms of class separation, the oblong TPU material is more spread out along the positive z-axis and both positive, and negative y-axis. Whereas the oblong rubber material is more compact and closed in. The range of displacement in the materials are evidently different as well. The TPU displays a wider range in both the X and Y directions, suggesting that the material is more flexible, while showing higher displacement along the z-axis, with values reaching up to 0.5. As for the rubber material, the displacements are tightly packed, indicating there is restricted movement and that the material is stiffer compared to its flexible counterpart. The cluster density of the material is different as well. The rubber cluster is dense and centred near the origin, whereas the TPU cluster is more dispersed. Linear Discriminant Analysis is a dimensionality reduction technique, much like PCA. The difference is that LDA maximises separability between categories of data. The technique is carried out by constructing within-class and between-class scatter matrices, then combining the two. That is later used to compute the eigenvalues and eigenvectors, which is then used to create a feature vector to project the data.

Figure 12 shows the LDA application to all 2D combinations of D_x, D_y, D_z,

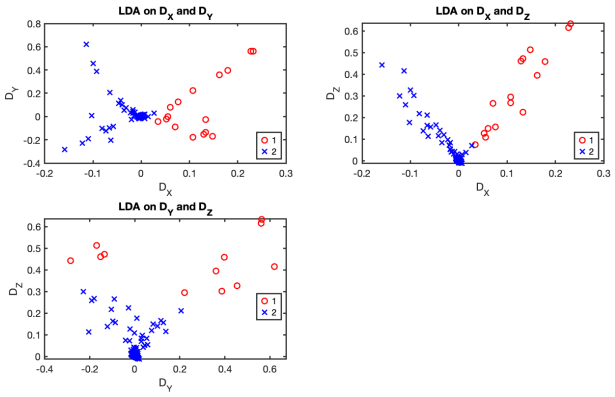

Figure 12: LDA application of D_x,D_y,D_z

with each plot showing a comparison. For the top-left plot, LDA is applied on D_x and D_y. Like the plot in figure 11 the oblong TPU material is spread out and the rubber material is compact and densely packed. There is a noticeable overlap between the classes. So that means the LDA applied between D_x and D_y isn't strong enough as there is a bit of an overlap between them, and doesn't

provide strong discrimination between them.

For the top-right plot, LDA is applied on D_x and D_z. Compared to the top-left plot, there is a much clearer separation between the two materials, with the red dots being spread out and blue dots being densely packed. LDA is more effective here because D_z introduces a strong variance between classes, especially vertically. The distribution shows that combining D_x with D_z improving class separation.

For the bottom plot, LDA is applied to D_y and D_z. As seen there is much clearer separation as the red points are well separated from blue points, showing very minimal overlap. The combination between D_y and D_z has provided the best separation among the three plots.

The key takeaway from this is that LDA is most effective when D_z is involved, as it contributes more variance between classes. Figure 13 shows the 3D tac-

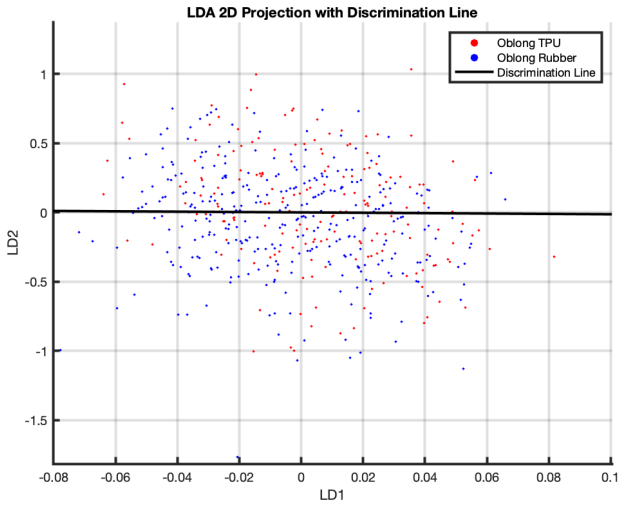

Figure 13: The 2D plot of the tactile displacement data with a discrimination line

tile displacement being reduced to two dimensions and re-plotted along with a discrimination line and two LDs, the primary linear displacement on the x-axis and secondary linear displacement on the y-axis. The primary linear displacement maximises the separation between the two classes. Whereas the secondary linear displacement captures additional variance that couldn't be explained by the primary linear displacement. The TPU peak data points are mostly located around the right-hand side of the LD1 (x-axis) with the values being close to 0. Whereas the rubber peak data points are spread out towards the left-hand side, with some of the points extending along negative LD1 values. The discrimination line separates most of the TPU and rubber points, indicating that LDA has found a boundary to classify the materials.

Figure 14 shows the tactile displacement data being projected in 3D. Like its 2D counterpart, the peak data from both materials are separated, with the noise being clustered near the origin. The discrimination plane separates the oblong TPU and rubber peak data,with the TPU being on the left side and rubber being on the right side. The discrimination plane indicates that LDA has captured the key differences in the behaviour of their displacements. The axes in the 3D plane, displacement X, Y and Z, represent the transformed feature space after LDA.

Using the 2D and 3D LDA plots provided, it shows that the TPU forms a tighter cluster near the decision boundary. This suggests that TPU exhibits consistent, predictable deformation under applied forces, leading to less variance in displacement readings. The tight cluster of the TPU plot represents the material's high elasticity, flexibility, and energy absorption. As for the rubber material, the plots show that the peak data points are more widely spread. This indicates greater variability in deformation, this is due to non-linear stiffness under stress.

D. Clustering and Classification

For this exercise, the oblong objects were chosen as the data from the central papillae. The materials of the object, PLA, rubber and TPU, are used to create a

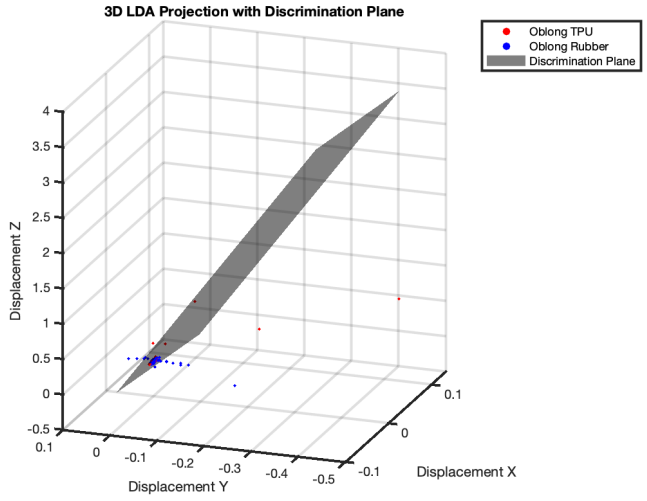

Figure 14: 3D projection of the LDA data

scatter plot. Once the object has been plotted, a clustering algorithm is applied and see whether the clusters correspond to the real-life outcomes.

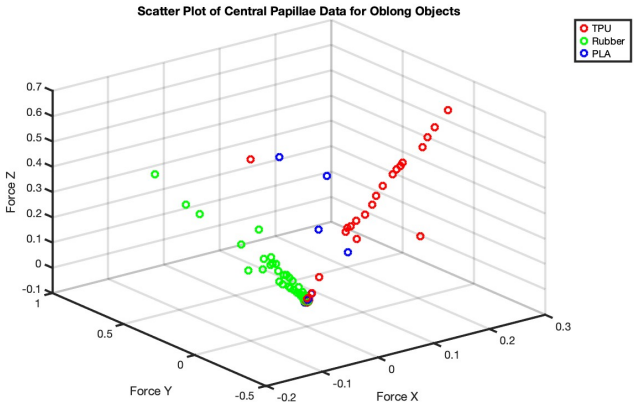

Figure 15: Scatter plot of central papillae data for oblong objects

Figure 15 shows the scatter plot of the central papillae data for the three materials of the oblong objects, with TPU stretching the furthest of all materials. Now that the scatter plot has been created, the next thing to do is to apply the clustering algorithm. The clustering algorithm chosen was k-means clustering. K-means clustering is a technique used in machine learning to group similar data points into clusters. So, the peak data from the oblong objects, will be grouped into clusters.

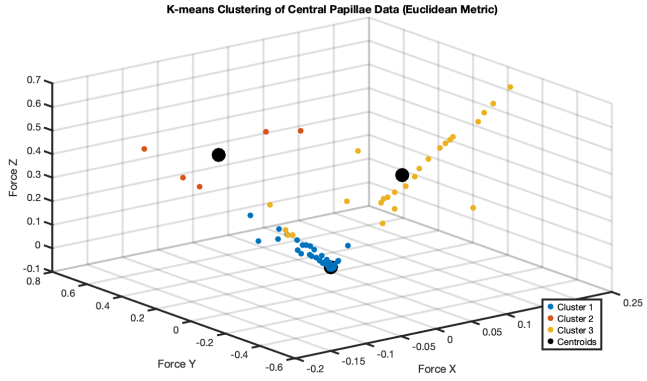

Figure 16: K-means Clustering of Central papillae Data (E.Metric)

Figure 16 shows the clustering of central papillae data, using k-means clustering. As seen on the plot, the clustering doesn't correspond well to real-life

outcomes. The reason why is because the 3d plot shows the three materials going out in separate lines, straying away from the centroids. Clustering won't be effective as it is supposed to group data together, instead it's straying further away from each other. Next is to see if changing the distance metric will improve the performance of the clustering.

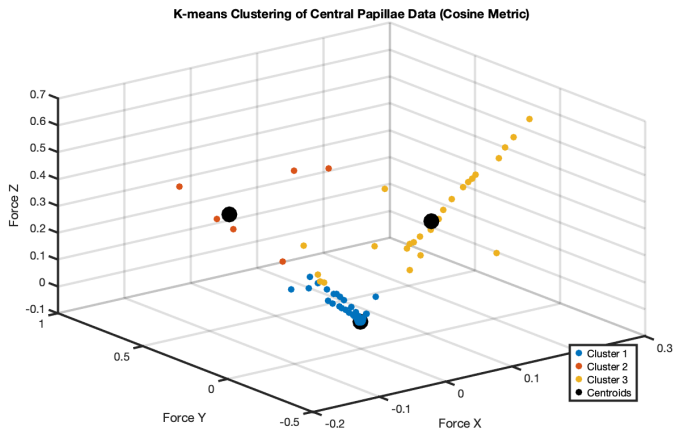

Figure 17: K-means Clustering of Central Papillae Data (C.Metric)

Figure 17 shows the clustering of the central papillae data using a cosine metric. There isn't much of a change in clustering, it still faces the same issue as the one in figure 16 that the materials aren't being grouped.

Bootstrap aggregation, or bagging, is the learning method that is used to reduce variance within a noisy data set. It is used to improve model accuracy and stability. A big contribution to that is decision Trees and confusion matrices.

For this project, the number of decision trees used is 3. The reason why is that the computer can only handle a small amount. Any more will increase the duration of the bagging training. Also, three trees provided the best results, as the accuracy on the classification of the data decreases as the tree increases.

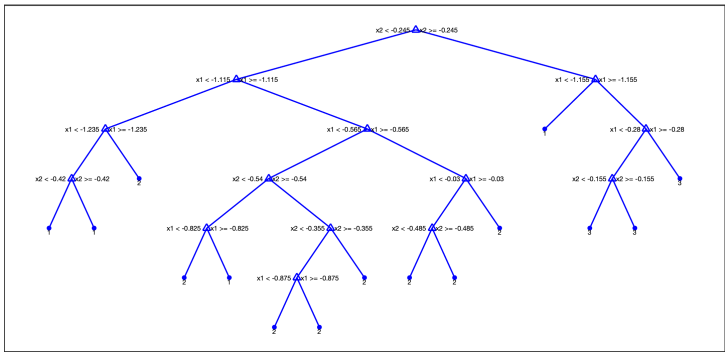

Figure 18: Class tree 1

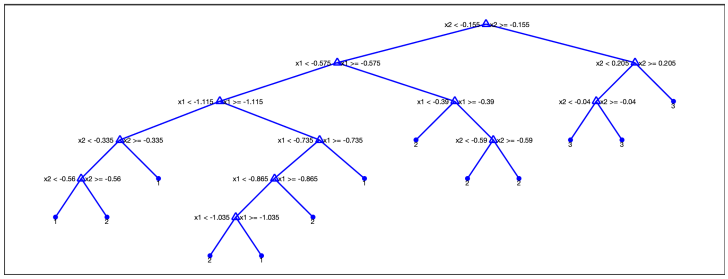

Figure 19: Class tree 2

Figure 18 and 19 show visualisations of two of the classification trees. Both trees have nodes that are tests on the data, with each branch being the outcome and the leaf node being the final decision and the pre-defined classes. In this case, the pre-defined classes are the materials.

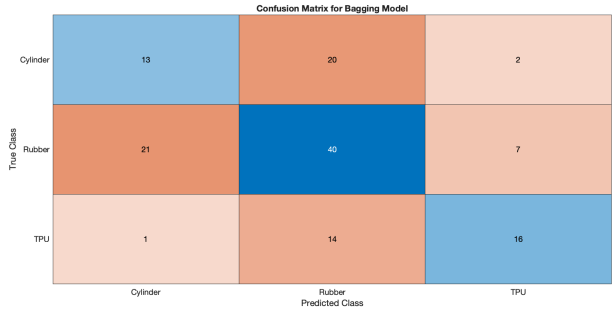

Figure 20: Confusion Matrix

Figure 20 shows the confusion matrix of the true class and the predicted class of the materials of the oblong objects. The confusion matrix often evaluates classification performance by showing how well a model correctly predicts different classes. In this case, the confusion matrix of the oblong object's materials is 51.4925%. This means that the confusion matrix can only produce around 51.5% predictions of the classes of the oblong object.

The misclassification in the results can be explained through the confusion matrix. As mentioned earlier, the confusion matrix can be used to evaluate the classification performance on the basis of correct predictions of each class. The PCA helped by reducing the model to 2 dimensions, giving a better visualisation of classification results, understanding why misclassification occurs, and improving feature selection.

E. Conclusion

The application of Principal Component Analysis (PCA) revealed that the tactile force data from the middle papillae could be effectively reduced to two dimensions while retaining key information about the material. This dimensionality reduction allowed us to observe clear separations between different materials, suggesting that PCA is useful for feature extraction.

Linear Discriminant Analysis (LDA) was used to differentiate between two objects of the same shape but made of different materials. The results demonstrated that the displacement data could be effectively used for classification, with clear boundaries found between the classes. The 3D LDA plot further highlighted the distinct tactile response patterns for different materials, particularly when displacement along the Z-axis was involved.

Clustering techniques such as k-means provided limited success in separating object classes based on tactile data, likely due to the underlying complexity, variability and shape of the dataset. Bagging was then applied to enhance classification stability, improving the overall model accuracy and reducing variance. Despite this improvement, some misclassifications persisted, which can be attributed to the overlapping tactile response patterns among certain materials.

Overall, these pattern recognition techniques have shown that it is feasible to distinguish objects based on tactile data, but I would argue that due to the similarity of each object's tactile response and the fact the various methods still had some accuracy, that it could be quite tricky to distinguish objects by touch.

However, our current analysis treats all contacts as equivalent, which may overlook valuable temporal information. One potential improvement could be to segment the data by contact regions or time intervals, allowing for a more nuanced analysis. While this approach may enhance classification performance, it would also increase computational complexity and require additional preprocessing.

Additionally, the analysis was conducted at a single time step for each contact. Incorporating the full time-series data could provide insights into the dynamics of the contact forces and displacements, enabling the detection of temporal patterns. This approach could significantly improve classification accuracy by capturing object interaction behaviour over time. However, it also introduces challenges such as increased data dimensionality and the need for more sophisticated temporal models.

In conclusion, this coursework showed that combining feature extraction, dimensionality reduction, and classification methods provides insights into tactile responses, laying a foundation for future work in robotic tactile sensing.